Dynamic magnetic phenomena in fine-particle goethite

S. Bocquet, R. J. Pollard, and J. D. Cashion
Department of Physics, Monash University, Clayton, Victoria 3168, Australia
(Received 17 December 1991; revised manuscript received 27 April 1992)

The distinctive Mössbauer spectra of fine-particle goethite (α-FeOOH) have been attributed by many authors to superparamagnetism. However, measurements of the magnetic anisotropy energy and particle volume show that the superparamagnetic blocking temperature for most samples is much greater than the Néel temperature. A model involving magnetic ordering of clusters created by high concentrations of vacancy defects is proposed, in which the cluster moments slowly relax, thus producing a Boltzmann distribution in the z component of the magnetization. The model provides excellent fits to the temperature-dependent hyperfine-field distributions observed in the Mössbauer spectra, and may have wider applicability to other diamagnetically substituted iron oxide materials. A linear relation is observed between T_N and the inverse mean crystallite dimension in the [111] direction of $-1060(130)$ K nm, and it is shown that goethite particles must have a volume of less than 1000 nm^3 in order to show superparamagnetic Mössbauer spectra at room temperature.

I. INTRODUCTION

The Mössbauer spectra of fine-particle goethite (α-FeOOH) show a temperature-dependent, asymmetric, magnetic hyperfine-field distribution, and have led some authors to conjecture that dynamic magnetic phenomena are present. The hyperfine splitting disappears at temperatures lower than the Néel temperature, T_N, of the bulk material (400 K).[1] Mössbauer results have led to inferences of superparamagnetism, without[2–5] or with[6] interparticle exchange interactions. However, analyses assuming superparamagnetism lead[2,4] to anisotropy energies in the range 400–1800 J m^{-3}, whereas the anisotropy energy for bulk goethite is at least 18 600 J m^{-3} (in as much as the spin-flop field is larger than 10 T),[7] and is expected[8] to be even greater for fine particles because of enhanced shape and surface contributions.

A recent study[9] using neutron-diffraction, Mössbauer spectroscopy, and SQUID magnetization measurements showed that T_N for fine particles is reduced from the bulk value (by 42 K in one particular sample, L20h), so that the disappearance of hyperfine splitting is likely to be directly associated with paramagnetism rather than with superparamagnetism.

Experiments described here confirm that the magnetic anisotropy is not reduced in fine particles. Further, because this large anisotropy and the reduced T_N are inconsistent with existing models, a new explanation of the magnetic relaxation behavior, which would also account for the hyperfine-field distribution, is required. A cluster ordering model is proposed in which the observed hyperfine-field reductions arise from slowly relaxing cluster moments. Mössbauer spectra of many fine-particle and disordered materials resemble those of goethite fine particles, so the model may be widely applicable.

II. EXPERIMENTAL

Goethite samples from a variety of sources were studied (Table I). All samples are synthetic except for a well-crystallized sample from the Harz Mountains in Germany and a poorly crystallized sample from Huy in the Belgian Ardennes. Analysis of the natural samples for aluminum content, by inductively coupled plasma emission spectroscopy, provided upper limits of 0.8 and 6 at. % Al for the Harz and Huy samples, respectively.

Transmission electron microscopy (TEM) was carried out with a JEOL JEM-200CX microscope operating at 80 kV, and permitted measurement of the average length (c axis) and width (b axis) of the particles. The thickness (a axis) could not be reliably measured. The Huy and VIII2 samples showed broad particle size distributions as well as large (Huy) or small (VIII2) amounts of amorphous material; all the other samples had narrow particle size distributions.

X-ray-diffraction (XRD) data were obtained using Fe $K\alpha$ and Co $K\alpha$ radiation. Linewidths were determined by least-squares fitting of pseudo-Voigt profiles, and the mean crystallite dimensions (MCD) were calculated from the Scherrer formula. $l^{\mathrm{MCD}}_{(100)}$ could not be determined directly, because the only diffraction peak for this direction, the (200) peak, is very weak. Instead, it was determined from a polar diagram of crystalline size in the ab plane, using the (010), (140), (130), (120), and (110) peaks.[10] The average particle thickness (a axis) was estimated as $(l^{\mathrm{MCD}}_{(100)}/l^{\mathrm{MCD}}_{(010)}) \times$ average width (b axis) for use in calculating the average particle volume. Details of sample characterization are given in Table I.

Constant acceleration Mössbauer spectrometers and ^{57}CoRh sources were used. Calibration is with respect to α-Fe at room temperature. Absorbers were prepared by mixing goethite powder with boron nitride and pressing in plastic holders.

TABLE I. Details of goethite samples.

Sample[a]	Particle length (nm)	Particle width (nm)	Particle volume (nm^3)	$l^{MCD}_{(100)}$ (nm)	$l^{MCD}_{(010)}$ (nm)	$l^{MCD}_{(001)}$ (nm)	$l^{MCD}_{(111)}$ (nm)	T_N (K)
Harz (Refs. 4, 29, 56, and 57)	704	455	1.46×10^8	115	115	42	100	398
PG1 (Ref. 58)	282	34	2.03×10^5	48	77	63	59	384[b]
GNL	557	33	3.51×10^5	24	41	33	39	380[b]
CG (Refs. 4, 23, 56, 57, and 59)	72.4	15.9	8 730	20	41	57	31	364[b]
L20h (Ref. 9)	48.7	11.8	3 590	19	28	44	31	358
DG60 (Refs. 4, 23, 56, and 57)	295	16	35 200	20	43	46	33	359[b]
DG4 (Refs. 4, 23, 56, and 57)	182	11.5	9 340	16	42	48	24	347
S1 (Refs. 6 and 10)[c]	24	12	1 980	12	21		16	324
VII2	144	28.6	30 400	12	47	42	21	353[b]
V2	131	14	10 600	12	30	34	21	360[b]
VIII2	136	19.5	21 600	11	27	37	16	337[b]
Huy	30	5.1	620	27	35	36	31	286[b]
GPC0B	34	4.4	220	11	33	35	16	261[b]
GPC0A			~160	13	21	25	21	280[b]

[a]The Harz and Huy samples are natural; the others are synthetic. References give details of preparation as well as results from each sample. Where no reference is given, the synthetic samples were prepared as described in Ref. 60.

[b]Determined from a single hyperfine-field data point.

[c]Particle dimensions and MCD data for the S1 sample obtained from Refs. 6 and 10.

III. DETERMINATION OF ANISOTROPY AND EXCHANGE FIELDS

The anisotropy field was determined by simultaneous fitting of Mössbauer spectra of sample DG4 in applied fields with a mean-field model[11] (Fig. 1). This gives an anisotropy field B_a of 0.423(11) T, or an anisotropy energy density $K=4.57(12)\times10^4$ J m^{-3}. A spin-flop field $B_{sf}\approx\sqrt{2B_aB_e}$ of 15.0 T is predicted, which is consistent with the observation that it is greater than 10 T for bulk goethite.[7]

The blocking temperature for superparamagnetism can be calculated from $T_B=KV/k\ \ln(\tau_m/\tau_0)$, where V is the particle volume, k is Boltzmann's constant, τ_m is the time scale of the experiment, and τ_0 is the correlation time of the fluctuations. For the 38-T hyperfine field of well-crystallized goethite at room temperature, $\tau_m=2.2\times10^{-8}$ s.

Estimating τ_0 presents some difficulty. Several authors[12–14] have suggested simply assuming a value of 10^{-12} or 10^{-11} s. Reid, Dickson, and Jones[15] determined $\tau_0=1.9\times10^{-10}$ s for horse spleen ferritin, a material which is similar to goethite. According to Brown's theory,[16–18] τ_0 is proportional to the magnetization. For an antiferromagnet, it is not clear whether this should be the sum of the absolute sublattice moments[19] or the net particle moment.[13,20,21] In the former case we find $\tau_0=2.4\times10^{-11}$ s, and in the latter case $\tau_0=4.6\times10^{-14}$ s using the estimated[12,22] net particle moment (10^{-20} J T^{-1}) for DG4.

The different estimates of τ_0, combined with $KV/k=3.09\times10^4$ K for DG4, lead to blocking temperatures between 2400 and 6400 K. These are well above T_N, so that superparamagnetism will not be observed in the Mössbauer spectra. Even for magnetization measurements, taking $\tau_m=100$ s and $\tau_0=4.6\times10^{-14}$ s provides a lower limit of $T_B=880$ K, which is well above T_N. This means that the disappearance of the remanent magnetization at about 30 K (Ref. 23) cannot be attributed to the

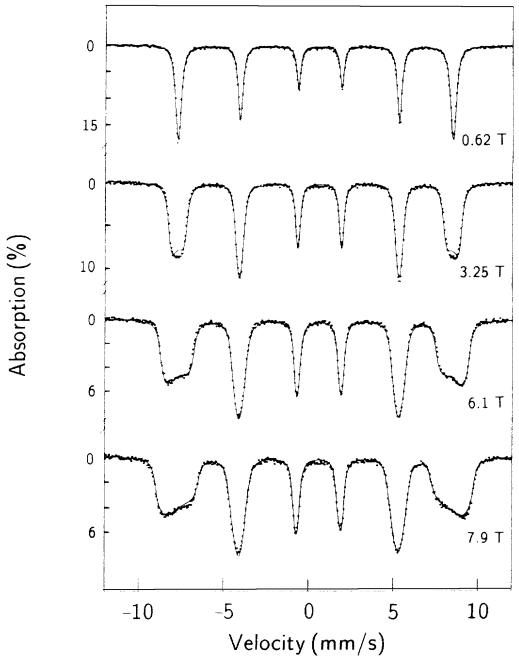

FIG. 1. Mössbauer spectra of DG4 goethite at 4.2 K in various applied magnetic fields. The spectra were fitted simultaneously to a mean-field model to determine the anisotropy field, and the solid lines show the fit.

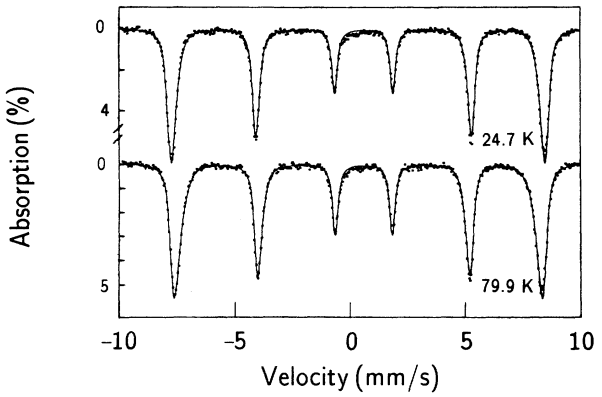

FIG. 2. Two low-temperature Mössbauer spectra of DG4 goethite. The solid lines show the fit using $p(B)$ as given by Eq. (1).

unblocking of superparamagnetic fluctuations throughout the particle volume.

At temperatures above 4.2 K an asymmetric hyperfine field distribution $p(B)$ is seen (Fig. 2). By taking B to be proportional to the z component of the iron magnetic moment, which is considered to be precessing rapidly about the z axis, $p(B)$ may be expressed as a Boltzmann distribution of precession angles θ:

$$B=B_0\cos\theta\ ,$$
$$p(B)\propto\exp(E_c\cos\theta/kT)\ ,\quad |B|\le B_0\ , \tag{1}$$
$$p(B)=0\ ,\quad |B|>B_0\ ,$$

where B_0 is the hyperfine field for $\theta=0$ and E_c is the height of a potential barrier in the form $E_c\cos\theta$. Models of slow superparamagnetic relaxation appear similar to this formulation,[5,24–27] however, here the potential barrier is associated with cluster exchange interactions.

For temperatures up to about 200 K, excellent fits are obtained by allowing B_0 and E_c to vary (Fig. 2). A plot of B_0 versus T^2 (Fig. 3) confirms that the spin-wave law for antiferromagnets applies. The exchange constant J is obtained from $J/k=\sqrt{B_0(0)C/m}$, where $B_0(0)$ is hyperfine field at 0 K, C is the spin-wave dispersion constant, and m is the slope of the line in Fig. 3. Spin-wave theory for an antiferromagnet[28] with spin $S=\frac{5}{2}$ and six nearest-neighbor magnetic ions in the lattice gives[29] $C=1.589\times10^{-3}$. If T_N (which is 347 K for DG4 and 400 K for bulk material) is reduced because of a dilution by vacancies, C will be similarly reduced. The Fe^{3+} ion concentration in the lattice, p, is estimated from the limiting slope $T_N^{-1}dT_N/dp=1.37$ for a simple-cubic lattice[30] as $p=0.903$. The limiting slope $C^{-1}dC/dp=1.78$ (Ref. 30) gives $C=1.314\times10^{-3}$. For DG4, it follows that $J/k=12.0(3)$ K, hence, $B_e=2JzS/g\mu_B=267(7)$ T which is the value used earlier to estimate B_{sf}.

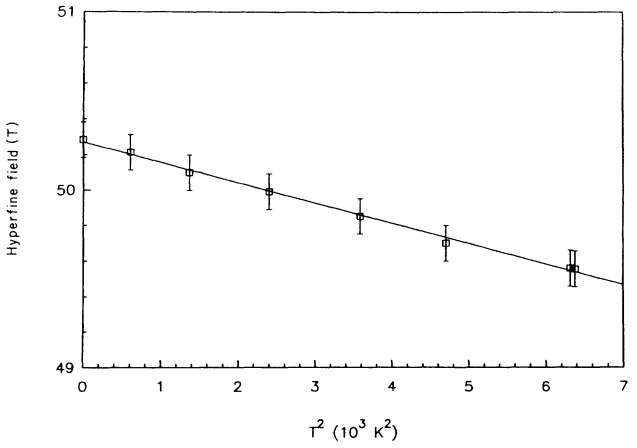

FIG. 3. Fit of the maximum hyperfine field B_0 for DG4 fine-particle goethite to the spin-wave law for an antiferromagnet.

IV. TEMPERATURE DEPENDENCE OF THE MÖSSBAUER SPECTRA

As the temperature is raised above 200 K, Eq. (1) becomes less adequate as a representation of the observed field distribution. This is due to the sharp cutoff at the high-field end of $p(B)$ becoming more rounded. If a Gaussian distribution for B_0 is introduced then the full

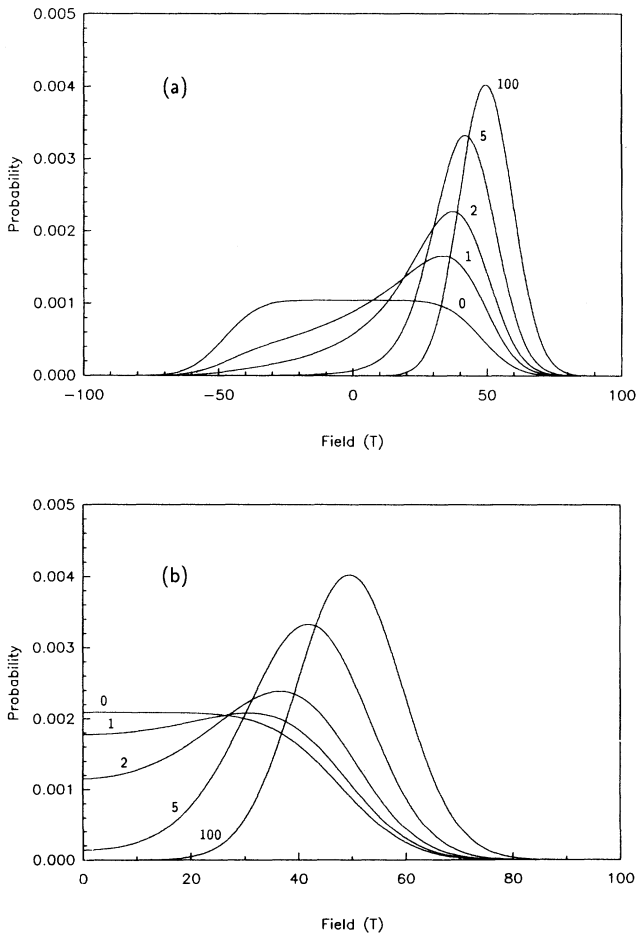

FIG. 4. Hyperfine-field distributions (a) $p(B)$ and (b) $p(|B|)$ calculated with $B_0=50$ T and $\sigma(B_0)=10$ T. The values of E_c/kT are marked on each curve.

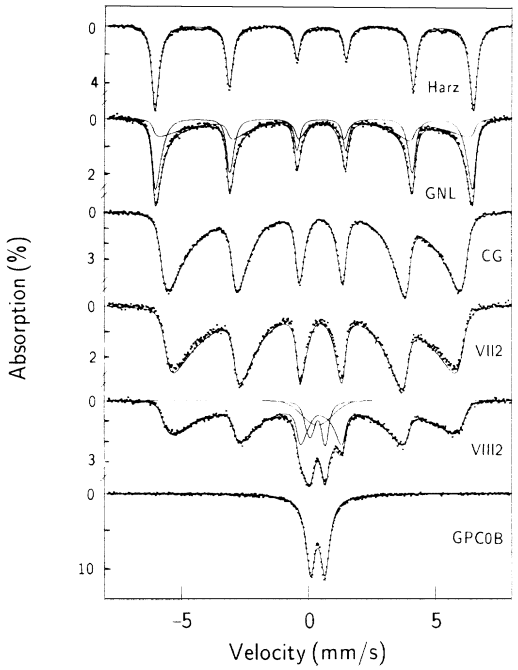

FIG. 5. Room-temperature Mössbauer spectra of goethites of differing particle sizes. The hyperfine-field distribution in Fig. 4 was used to fit the spectra.

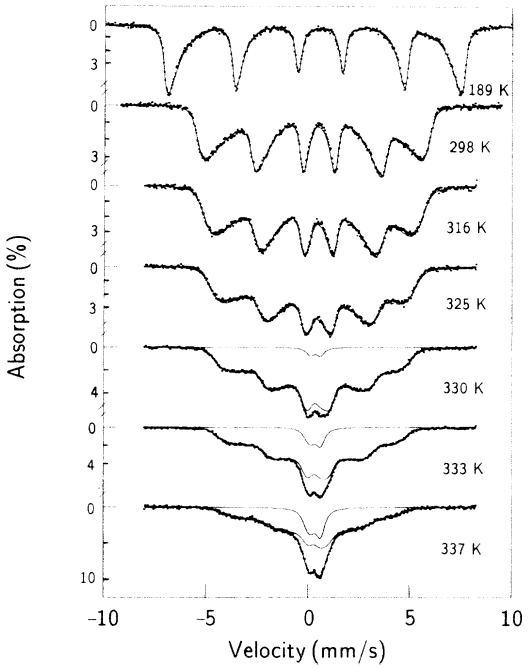

FIG. 6. Mössbauer spectra of DG4 at various temperatures, fitted using $p(B)$ in Fig. 4.

hyperfine-field distribution $p(B)$ is characterized by three parameters: $\langle B_0 \rangle$ (hereafter denoted simply B_0), the standard deviation $\sigma(B_0)$, and E_c/kT. A representative form is shown in Fig. 4. Good fits were obtained, as seen in Fig. 5 for room-temperature spectra. The line positions and relative intensities for each subspectrum were calculated from the full Hamiltonian for an axially symmetric electric-field gradient (EFG) with V_{zz} perpendicular to B.

Two components, with different values of E_c, were needed to fit the spectrum of sample GNL, presumably because of a distribution in E_c. Only the relative area and E_c were varied independently for the second component; the other parameters were set equal to the corresponding ones for the first component. In the case of VIII2, it was necessary to also introduce separate doublet and Gaussian components. The Gaussian component is an empirical representation of that part of the spectrum due to particles with superparamagnetic relaxation times comparable to τ_m. The room-temperature spectrum of GPC0B is a simple doublet, indicating that this sample is entirely paramagnetic or superparamagnetic.

Spectra of DG4 at various temperatures are shown in Fig. 6. Close to T_N it is necessary to introduce a separate doublet into the fit but a Gaussian component is not required at any temperature. The coexistence of a doublet and a hyperfine-field distribution is attributed to a distribution in T_N.

The results are summarized in Table II. Note the ex-

TABLE II. Parameters derived from Mössbauer spectra of DG4 goethite.

Temperature (K)	Γ[a] (mm s^{-1})	Isomer[b] shift (mm s^{-1})	$\frac{1}{2}eQV_{zz}$[b] (mm s^{-1})	Doublet area (%)	B_0 (T)	$\sigma(B_0)$ (T)	E_c (K)	$\langle B \rangle$[c] (T)
4.2	0.34	0.48	0.48	0	50.2	0.0		50.2
189	0.31	0.42	0.50	0	45.2	0.2	2490	41.5
298	0.31	0.37	0.51	0	34.7	1.1	1200	27.0
316	0.41	0.36	0.50	0	32.3	1.7	1020	23.6
325	0.44	0.35	0.52	0	30.1	1.9	744	19.9
330	0.44	0.34	0.48	2.8	28.7	1.8	488	16.8
333	0.46	0.34	0.49	8.5	28.0	1.8	356	14.7
337	0.48	0.34	0.51	18	26.5	4.0	175	12.6
351	0.46	0.33	0.50	100				0.0

[a]Full linewidth at half-maximum intensity.
[b]Constrained to be equal for doublet and hyperfine split components where applicable.
[c]Obtained from model-independent fits.

pected increase in $\sigma(B_0)$ near T_N. Values of $\langle B \rangle$ obtained using a model-independent fitting method[31] are included for comparison.

V. ORDERING MODEL

The next step is to specify a model which will give a physical interpretation to $p(B)$. Figure 7 shows the hyperfine field data for well-crystallized natural goethite, which is not well fitted by the Brillouin function for $S=\frac{5}{2}$. For Fe^{3+}, the hyperfine field, $B^b(T)$, is proportional to the sublattice magnetization $M^b(T)$, where both symbols refer to the bulk material. A good fit is obtained by incorporating the order parameter to the power $\frac{3}{2}$, thereby changing the critical exponent from $\frac{1}{2}$ to $\frac{1}{3}$, resulting in

$$\left[\frac{M^b(T)}{M^b(0)}\right]^{3/2}=\mathcal{B}_s\left[\frac{3ST_N^b}{(S+1)T}\left[\frac{M^b(T)}{M^b(0)}\right]^{3/2}\right], \quad (2)$$

where T_N^b is T_N for bulk (well-crystallized) material, and $\mathcal{B}_s$ is the Brillouin function. The values $B^b(0)=50.74$ T and $T_N^b=398.1$ K were deduced. An expression for E_c in terms of T_N is obtained from mean-field theory:[6]

$$E_c(T)=3kT_N[M^b(T)/M^b(T_N)]^2\overline{M}(T)/M^b(0) . \quad (3)$$

$\overline{M}(T)$ is obtained from

$$\left[\frac{\overline{M}(T)}{M^b(0)}\right]^{3/2}=\mathcal{L}\left[\frac{3T_N}{T}\left[\frac{M^b(T)}{M^b(T_N)}\right]^2\left[\frac{\overline{M}(T)}{M^b(0)}\right]^{3/2}\right], \quad (4)$$

where $\mathcal{L}$ is the Langevin function. Equation (4) corresponds to Eq. (11) of Ref. 6 with $b(T)=\overline{M}(T)/M^b(0)$, except that we evaluate the mean-field theory in $b(T)^{3/2}$ rather than $b(T)$.

The model was checked against experiment in three ways (Fig. 8). First, the temperature variation of E_c to Eq. (3) was fitted for three samples [Fig. 8(a)]. T_N was the only free parameter. The agreement is rather poor; in particular Eq. (3) underestimates the low-temperature value of E_c. However, it is well known that mean-field theory overestimates T_N for a given strength of exchange interaction.[32] In the classical limit, an empirical formula[33] leads to an exchange energy 40% larger than predicted by mean-field theory, and the fit for E_c errs by about this much at 4.2 K. The fit is the worst at low temperatures, but because $p(B)$ is least sensitive to E_c here, we can still make use of Eq. (3) to calculate the temperature dependence of B_0.

The second check is the temperature variation of B_0 [Fig. 8(b)]. The hyperfine field of the Harz sample (which is well crystallized) is shown for comparison. B_0 for the other samples deviates from the Harz data as the temperature rises, the falloff being more rapid for smaller T_N values. The solid lines in Fig. 8(b) are given by the

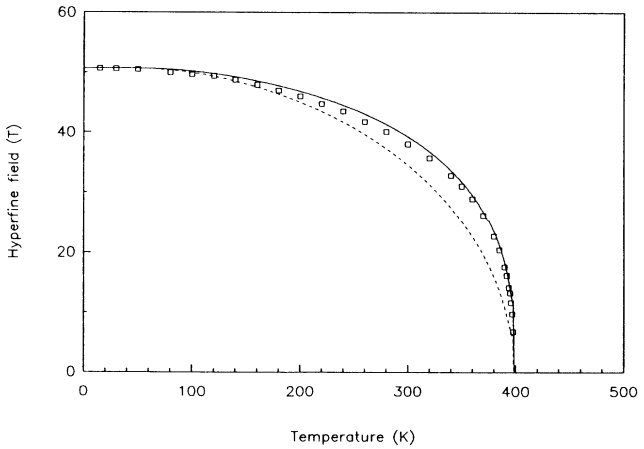

FIG. 7. Temperature dependence of the magnetic hyperfine field for the well-crystallized Harz sample (from Ref. 29). The solid line is a fit to a Brillouin function for $S=\frac{5}{2}$ modified as described in the text. Dashed line: unmodified spin-$\frac{5}{2}$ Brillouin function.

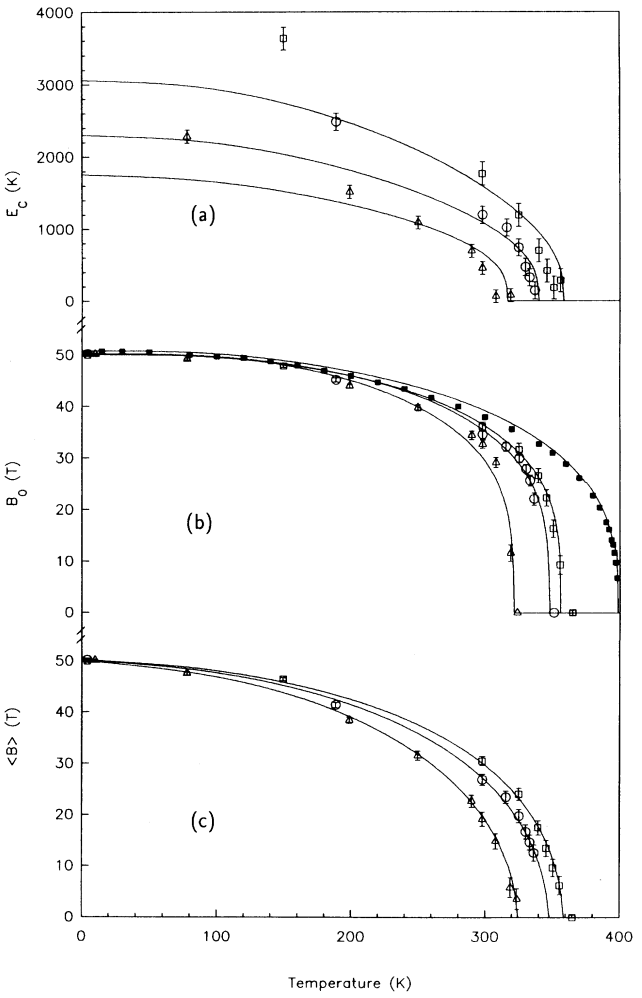

FIG. 8. Temperature dependence of (a) the cluster exchange energy E_c, (b) the maximum hyperfine field B_0, and (c) the average hyperfine field $\langle B \rangle$ for the S1 (△), DG4 (○), and L20h (□) samples. $B^b(T)$ for the Harz sample (■) is also shown in (b). Values of E_c and B_0 for DG4 were obtained from the fits shown in Fig. 6; values of $\langle B \rangle$ were obtained from model-independent fits. Solid lines are fits to the cluster ordering model.

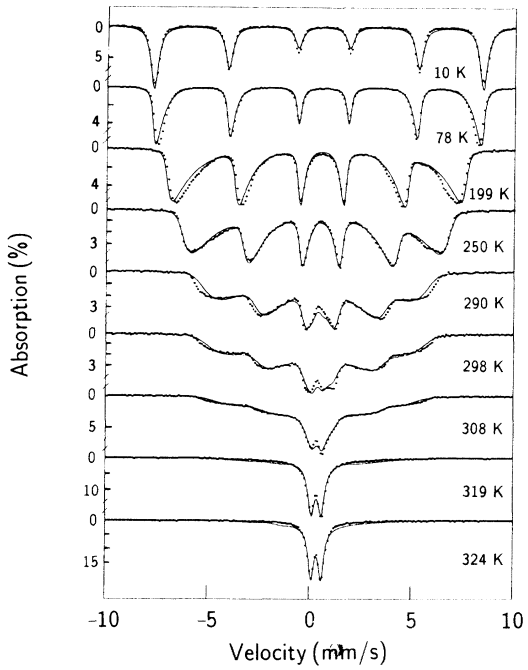

FIG. 9. Mössbauer spectra of S1 goethite at various temperatures (from Ref. 6). The solid lines are calculated using the cluster ordering model, with a Gaussian distribution of T_N.

thermal average of $B^b(T)$ over the cluster exchange potential E_c:

$$B_0(T)=B^b(T)\mathcal{B}_s\left[\frac{s}{s+1}E_c/kT\right] . \quad (5)$$

Third, the average hyperfine field is calculated [Fig. 8(c)] from

$$\langle B(T)\rangle = B_0(T)\mathcal{L}(E_c/kT) . \quad (6)$$

Values of T_N from these fits are given in Table III.

The final step is to use the complete model to compute Mössbauer spectra. Figure 9 shows the results for the S1 sample.[6] A Gaussian distribution of T_N with a mean of 319 K and a standard deviation of 13 K was used, and $B_0(0)$ was taken to be 50.1 T. It should be emphasized that once these parameters are specified, $p(B)$ for each temperature is calculated directly from the model, without introducing any further adjustable parameters. The EFG and isomer shift were fixed to values obtained from model-independent fits. The model is able to reproduce the experimental data remarkably well, with only small discrepancies. In particular, the Gaussian distribution of T_N is able to account for the broadening at the outer edge of $p(B)$.

VI. EFFECTS OF CRYSTALLINITY

Estimates of the Néel temperature have been made (Table III) for four samples. In order to obtain a simple estimate of T_N for the other samples, $\langle B\rangle$ was determined from model-independent field distribution fits to the room-temperature spectra. T_N (Table I) was then calculated from Eq. (6). Table III provides a comparison of the accuracy of the method for the four samples for which a full range of spectra was taken. For samples GPC0A, GPC0B, Huy, and VIII2, a spectrum at 150–200 K replaced the room-temperature spectrum.

Figure 10 shows the relation between T_N and $1/l^{\mathrm{MCD}}_{(111)}$. Excluding the three samples with T_N apparently less than 300 K, the relation is linear with a correlation coefficient of -0.91. T_N^b for bulk goethite obtained from the fit is 399(5) K, and the constant of proportionality is $-1060(130)$ K nm. If the particle shape is approximated by a rectangular prism, the specific surface area may be estimated as $(2/l^{\mathrm{MCD}}_{(100)}+2/l^{\mathrm{MCD}}_{(010)}+2/l^{\mathrm{MCD}}_{(001)})/\rho$, where ρ is the density (4.3 g cm^{-3}). A somewhat worse correlation of -0.84 was obtained between T_N and this quantity.

The critical volume V_c for superparamagnetism to be observed in the Mössbauer spectrum of goethite at room temperature can be estimated from the relationship $V_c \approx 13kT_B/\mathrm{K}$. For $T_B=298$ K and $K=45700$ J m^{-3}, this gives $V_c=1170$ nm.[3] Thus, the GPC0A, GPC0B, and Huy samples should be superparamagnetic at room temperature and this is consistent with their Mössbauer spectra, which are doublets. It was noted in Sec. IV that, in order to fit the Mössbauer spectrum of VIII2 at room temperature, it was necessary to include separate doublet and Gaussian components. These account for 13% of the total spectral area, indicating that a proportion of the sample is superparamagnetic on the time scale of Mössbauer spectroscopy. Electron micrographs of the sample confirmed the presence of some very finely divided material.

The effect of collective magnetic excitations on $\langle B\rangle$ can be calculated using the formula given in Ref. 34. For the S1, CG, and L20h samples, this produces a small correction to $\langle B\rangle$ ($\sim$0.2–1.1 T). For GPC0A, GPC0B, and Huy the correction is 2–9 T. For the other samples, the effect is negligible (0.1 T or less). It seems reasonable

TABLE III. Estimates of T_N (K). The number in parentheses is the uncertainty in the last digit.

	Sample			
Method	S1	DG4	L20h	Harz[a]
Fit to B_0 [Fig. 8(b)]	321(2)	347(2)	356(2)	398.1(3)
Fit to $\langle B\rangle$ [Fig. 8(c)]	324.3(6)	347(1)	358.0(9)	398.1(3)
Single temperature	333	346	360	394
Neutron diffraction (Ref. 9)			358(1)	

[a]For the Harz sample $B_0 \approx \langle B\rangle \approx B^b$, and the fit is shown in Fig. 7.

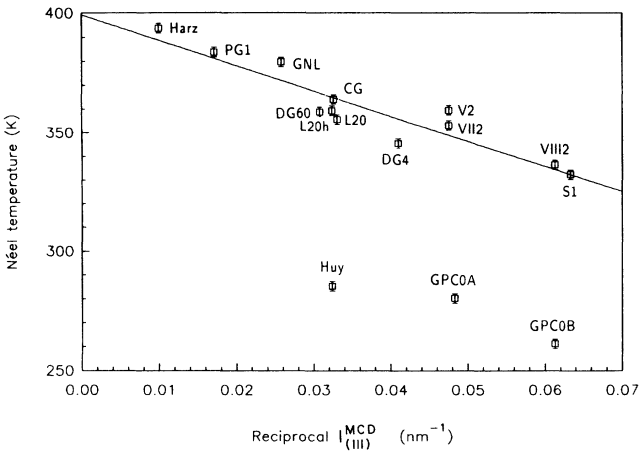

FIG. 10. T_N determined from the cluster ordering model vs reciprocal mean crystallite [111] dimension. The three samples with apparent $T_N < 300$ K were not included in the fit.

to attribute the anomalously low calculated T_N for the Huy, GPC0A, and GPC0B samples to the effect of collective magnetic excitations in reducing $\langle B \rangle$. The 6 at. % Al content of the Huy sample should also lower its T_N by about 43 K.[35]

VII. DISCUSSION

The hyperfine-field distribution has only three adjustable parameters, all of which have a physical interpretation: the Gaussian mean and standard deviation, and the cluster exchange potential. However, B_0 does not correspond to a readily identifiable feature of the field distribution, except in the limit $E_c/kT \rightarrow \infty$, where it is the maximum probability field, and in the limit $E_c/kT \rightarrow 0$, where it is the inflection point on the high-field end of the distribution (see Fig. 4).

Two distributions, with different exchange potentials, were needed to fit the Mössbauer spectra of GNL and PG1 at room temperature. These samples have relatively good crystallinity (T_N close to T_N^b). The cluster exchange energy E_c [Eq. (3)] diverges as $T_N \rightarrow T_N^b$ in the mean-field model, so a distribution in T_N will produce a much broader distribution in E_c if T_N is close to T_N^b. The need to use two values of E_c for these samples, but not for the others, is thus understood.

Our model differs from the superferromagnetic model of Ref. 6 in several ways. First, it considers each particle as being made up of interacting clusters with an ordering temperature T_N, whereas in the superferromagnetic model the particles as a whole interact with their neighbors. Second, it contains the critical exponent $\beta = \frac{1}{3}$ rather than $\beta = \frac{1}{2}$. Third, E_c is not simply proportional to $\langle M(T) \rangle$. The excellent fit to $\langle B \rangle$ achieved with the superferromagnetic model appears to result from a fortuitous cancellation between a reduction in the calculated values due to taking $\beta = \frac{1}{2}$ and an increase due to setting the cluster mean-field proportional to $\langle B \rangle$. The superferromagnetic model implies that the maximum hyperfine field at temperatures below T_N will be that of the bulk material, whereas this is clearly not the case [our Fig. 8(b) and Fig. 6 of Ref. 6)].

Our model assumes that, compared with τ_m for Mössbauer spectroscopy, the cluster relaxation is slow, and the relaxation of the individual Fe^{3+} ions is rapid. Selective excitation double Mössbauer experiments on fine-particle goethite show[36] relaxation at a rate comparable with τ_m close to T_N, the dominant relaxation process being a reversal of the ionic moment. However, the experimental data are reproduced remarkably well by the model (Fig. 9), so it is inferred that neglecting relaxation on the Mössbauer time scale is a good approximation.

The reduction of T_N is attributable to dilution by vacancy defects.[37–39] The evidence for such defects being present comes from two main observations. First, T_N is reduced for small crystallite sizes, and it is reasonable to expect that the defect concentration increases with decreasing particle dimensions. Second, the effect of small particle sizes on the Mössbauer spectra and magnetic properties is virtually identical to the effect of aluminum substitution.[40]

VIII. CONCLUSION

Anisotropy and exchange fields were measured for a sample of fine-particle goethite with $T_N = 347$ K. A blocking temperature of at least 2400 K for superparamagnetism to be observed in the Mössbauer spectrum was derived from the anisotropy field and the particle volume. The measured anisotropy shows that in samples with particle volumes greater than 1000 nm^3 the broadening of the Mössbauer spectrum does not result from superparamagnetism. A calculated blocking temperature of 880 K for magnetization measurements shows that the disappearance of the remanent magnetization at about 30 K cannot be attributed to superparamagnetism either.

A cluster ordering model is able to account for the form and temperature dependence of the Mössbauer spectra. The distinctive hyperfine-field distribution arises from slow relaxation of the cluster magnetization which produces a Boltzmann distribution in the z component of the magnetization. There is rapid relaxation between the Zeeman levels of the individual Fe^{3+} ions, resulting in a reduction of the maximum hyperfine field seen in the Mössbauer spectrum.

A survey of the literature reveals a large number of materials which have similar hyperfine-field distributions. These include aluminous goethite,[40] aluminous hematite,[41] substituted ferrites,[42] fine-particle ferrites,[43] fine particles of other iron oxides[44–47] and oxyhydroxides,[48–50] silicates,[51,52] iron vanadium oxide bronze,[53] and Invar alloys.[54,55] A common feature is magnetic frustration, produced by vacancies or diamagnetic ion substitution, or by competing exchange. The model may prove useful in interpreting the spectra of these materials.

T_N reduces linearly with $1/l^{MCD}_{(111)}$ with a slope of $-1060(130)$ K nm. This is attributed to the presence of vacancy defects, their concentration increasing with decreasing particle dimensions.

ACKNOWLEDGMENTS

We thank D. Brož and R. M. Cornell for supplying samples, E. De Grave for supplying samples and XRD patterns, and S. Mørup for Mössbauer spectra of the S1 sample. This work is funded by the Australian Research Council.

[1]J. B. Forsyth, I. G. Hedley, and C. E. Johnson, J. Phys. C **1**, 179 (1968).

[2]T. Shinjo, J. Phys. Soc. Jpn. **21**, 917 (1966).

[3]A. M. van der Kraan, Ph.D. thesis, Technische Hogeschool Delft, Netherlands, 1972.

[4]D. Brož, J. Strakova, J. Šubrt, J. Vinš, B. Sedlák, and S. I. Reiman, Hyperfine Interact. **54**, 479 (1990).

[5]V. E. Sedov, Hyperfine Interact. **56**, 1491 (1990).

[6]S. Mørup, M. B. Madsen, J. Franck, J. Villadsen, and C. J. W. Koch, J. Magn. Magn. Mater. **40**, 163 (1983).

[7]A. Meagher, Q. A. Pankhurst, and D. P. E. Dickson, Hyperfine Interact. **28**, 533 (1986).

[8]S. Mørup, J. A. Dumesic, and H. Topsøe, in *Applications of Mössbauer Spectroscopy,* edited by R. L. Cohen (Academic, New York, 1980) Vol. II, p. 1.

[9]S. Bocquet and S. J. Kennedy, J. Magn. Magn. Mater. **109**, 260 (1992).

[10]C. J. W. Koch, M. B. Madsen, S. Mørup, G. Christiansen, L. Gerward, and J. Villadsen, Clays Clay Miner. **34**, 17 (1986).

[11]Q. A. Pankhurst and R. J. Pollard, J. Phys. Condens. Matter **2**, 7329 (1990).

[12]L. Néel, J. Phys. Soc. Jpn. **17**, Suppl. B-I, 676 (1962).

[13]D. H. Jones and K. K. P. Srivastava, J. Magn. Magn. Mater. **78**, 320 (1989).

[14]D. H. Jones, Hyperfine Interact. **47**, 289 (1989).

[15]N. M. K. Reid, D. P. E. Dickson, and D. H. Jones, Hyperfine Interact. **56**, 1487 (1990).

[16]W. F. Brown, Phys. Rev. **130**, 1677 (1963).

[17]L. Bessais, L. Ben Jaffel, and J. L. Dormann, J. Magn. Magn. Mater. **104-107**, 1565 (1992).

[18]L. Bessais, L. Ben Jaffel, and J. L. Dormann, Phys. Rev. B **45**, 7805 (1992).

[19]G. N. Belozerskii and B. S. Pavlov, J. Magn. Magn. Mater. **12**, 34 (1979).

[20]J. L. Dormann, J. R. Cui, and C. Sella, J. Appl. Phys. **57**, 4283 (1985).

[21]J. L. Dormann, Rev. Phys. Appl. **16**, 275 (1981).

[22]R. J. Pollard, Q. A. Pankhurst, and P. Zientek, Phys. Chem. Miner. **18**, 259 (1991).

[23]D. Brož and B. Sedlák, J. Magn. Magn. Mater. **102**, 103 (1991).

[24]G. N. Belozerskii and S. Simonyan, J. Phys. (Paris) Colloq. **40**, C2-237 (1979).

[25]G. N. Belozerskii and B. S. Pavlov, Fiz. Tverd. Tela **25**, 1690 (1983) [Sov. Phys. Solid State **25**, 974 (1983)].

[26]A. M. Afanas'ev and V. E. Sedov, Izv. Akad. Nauk. Ser. Fiz. **50**, 2348 (1986).

[27]D. H. Jones and K. K. P. Srivastava, Phys. Rev. B **34**, 7542 (1986).

[28]R. Kubo, Phys. Rev. **87**, 568 (1952).

[29]E. De Grave and R. E. Vandenberghe, Hyperfine Interact. **28**, 643 (1986).

[30]A. B. Harris and S. Kirkpatrick, Phys. Rev. B **16**, 542 (1977).

[31]C. Wivel and S. Mørup, J. Phys. E **14**, 605 (1981).

[32]J. S. Smart, *Effective Field Theories of Magnetism* (Saunders, Philadelphia, 1966), Chap. 4.

[33]G. S. Rushbrooke and P. J. Wood, Mol. Phys. **1**, 257 (1958).

[34]S. Mørup, J. Magn. Magn. Mater. **37**, 39 (1983).

[35]J. Fleisch, R. Grimm, J. Grübler, and P. Gütlich, J. Phys. (Paris) Colloq. **41**, C1-169 (1980).

[36]M. V. Zelepukhin, V. E. Sedov, G. V. Smirnov, V. N. Dubinin, and O. N. Razumov, Pis'ma Zh. Eksp. Teor. Fiz. **49**, 143 (1989) [JETP Lett. **49**, 168 (1989)].

[37]G. W. van Oosterhout, *Proceedings of the International Conference Magnetism, Nottingham, 1964* (Institute of Physics and Physical Society, London, 1965), p. 529.

[38]N. Yamamoto, Bull. Inst. Chem. Res. Kyoto Univ. **46**, 283 (1968).

[39]F. van der Woude and A. J. Dekker, Phys. Status Solidi **13**, 181 (1966).

[40]S. A. Fysh and P. E. Clark, Phys. Chem. Miner. **8**, 180 (1982).

[41]E. De Grave, L. H. Bowen, D. D. Amarasiriwardena, and R. E. Vandenberghe, J. Magn. Magn. Mater. **72**, 129 (1988).

[42]E. De Grave, R. Vanleerberghe, C. Dauwe, J. De Sitter, and A. Govaert, J. Phys. (Paris) Colloq. **37**, C6-97 (1976).

[43]R. E. Vandenberghe, R. Vanleerberghe, and D. Gryffroy, Phys. Lett. **101A**, 297 (1984).

[44]S. Mørup, H. Topsøe, and J. Lipka, J. Phys. (Paris) Colloq. **37**, C6-287 (1976).

[45]E. Tronc and D. Bonnin, J. Phys. (Paris) Lett. **46**, L437 (1985).

[46]E. Tronc and J. P. Jolivet, Hyperfine Interact. **28**, 525 (1986).

[47]P. M. A. De Bakker, E. De Grave, R. E. Vandenberghe, L. H. Bowen, R. J. Pollard, and R. M. Persoons, Phys. Chem. Miner. **18**, 131 (1991).

[48]E. De Grave, R. M. Persoons, D. G. Chambaere, R. E. Vandenberghe, and L. H. Bowen, Phys. Chem. Miner, **13**, 61 (1986).

[49]R. M. Persoons, D. G. Chambaere, and E. De Grave, Hyperfine Interact. **28**, 647 (1986).

[50]M. B. Madsen, S. Mørup, C. J. W. Koch, and O. K. Borggaard, Surf. Sci. **156**, 328 (1985).

[51]G. Longworth, M. G. Townsend, and C. A. M. Ross, Hyperfine Interact. **28**, 451 (1986).

[52]E. Murad, J. D. Cashion, and L. J. Brown, Clay Miner. **25**, 261 (1990).

[53]H. Lass and J. Pebler, in *Industrial Applications of the Mössbauer Effect,* edited by G. J. Long and J. G. Stevens (Plenum, New York, 1986), p. 399.

[54]J. Hesse and E. Hagen, Hyperfine Interact. **28**, 475 (1986).

[55]J. Hesse, Hyperfine Interact. **47**, 357 (1989).

[56]D. Brož, A. Šolcová, J. Šubrt, B. Sedlák, F. Zounová, and S. I. Reiman, Acta Phys. Slov. **39**, 235 (1989).

[57]D. Brož, S. I. Reiman, and B. Sedlák, Hyperfine Interact. **60**, 1011 (1990).

[58]R. J. Pollard, Q. A. Pankhurst, and P. Zientek, J. Magn. Magn. Mater. **104-107**, 1557 (1992).

[59]R. M. Cornell and R. Giovanoli, Clays Clay Miner. **34**, 557 (1986).

[60]D. C. Golden, L. H. Bowen, S. B. Weed, and J. M. Bigham, Soil Sci. Soc. Am. J. **43**, 802 (1979).